

Electronic Structure and Fermi Surface Character of ZrCuSiAs Structured Superconductor: LaNiPO

Wei-Bing Zhang,^{1,2} Xiao-Bing Xiao,² Wen Li,² Wei-Yang Yu,² Na Wang,² and Bi-Yu Tang^{1,2,*}

¹*School of Chemistry and Chemical Engineering, Guangxi University, Nanning, 530004, China.*

²*Department of Physics and Key Laboratory of Low Dimensional Materials & Application Technology of Ministry of Education, Xiangtan University, Hunan Province, 411105, China.*

Based on First-principles calculation, we have investigated electronic structure of a ZrCuSiAs structured superconductor LaNiPO. The density of states, band structures and Fermi surfaces have been given in detail. Our results indicate that the bonding of the La-O and Ni-P is strongly covalent whereas binding property between the LaO and NiP blocks is mostly ionic. It's also found that four bands are across the Fermi level and the corresponding Fermi surfaces all have a two-dimensional character. In addition, we also give the band decomposed charge density, which suggests that orbital components of Fermi surfaces are more complicated than cuprate superconductors.

PACS numbers: 71.18.+y, 71.15.Mb, 74.25.Jb

I. INTRODUCTION

Quaternary rare earth transition metal phosphide oxides with the tetragonal ZrCuSiAs structure¹ are known for more than twenty years². Numerous quaternary phosphide oxides have been reported, including the actinoid and copper-containing compounds UCuPO,³ ThCuPO⁴ as well as the series of lanthanoid (Ln) compounds LnFePO², LnRuPO², LnCoPO², LnOsPO, LnZnPO^{5,6} and LnMnPO⁷.

However, most of interests are limited to the synthesization and structural analysis, only few physical properties have been investigated for this compound series. Because of open-shell structure and electronic correlation of 3d electrons, the ZrCuSiAs type transition metal phosphide oxides are expected to display interesting magnetic and electronic phenomena. With the same crystal structure, the different groundstates including antiferromagnetic insulator⁸, semiconductor and metal⁶ have been found in the ZrCuSiAs type compounds. Moreover, LaFePO^{9,10} has been found to be a type II superconductor with T_c of 3.2~6.5 K, which leads to renewed interest in studying physical properties in this class of materials. Ferromagnetic Kondo lattice systems found in Ce-based phosphide oxides CeTPO (T=Ru,Os)^{11,12} also attract much attentions.

Recently, a new compound LaNiPO with ZrCuSiAs structure has been reported by Watanabe *et al.*¹³, and it has also been synthesized by Tegel *et al.*¹⁴ with different experimental method. Moreover, it has been identified as a superconductor with a critical temperature T_c of 3 and 4.3 K, respectively. Moreover, LaNiPO is the first nickel phosphide oxide and the second superconducting compound in LaMPO (M=transition metal). It seems that the superconductivity may be a common phenomena in this family. Although this T_c is lower than that of the copper oxides, because of possible different underlying mechanism, the discovery of superconductivity in the new material systems can provide valuable knowledge for understanding of superconduction and for finding another superconductor. Thus, it is crucial to clarify the underlying mechanism of novel superconductivity in this series of compounds. Whereas the understanding of electronic structure especially the Fermi surface character is a basic step to obtain insight into the superconductivity mechanism.

In present calculation, we perform the systematic investigation for LaNiPO based on density functional theory. The detailed structural parameters, electronic structures and Fermi surfaces were given. The bonding properties are also discussed in combination with the concept of two-dimensional (2D) building blocks and a Bader analysis of the charge density. The band decomposed charge density is also provided to analyze the orbital character of each Fermi surface.

II. COMPUTATIONAL DETAILS

The present calculations have been performed using the Vienna Ab initio Simulation Package (VASP) code^{15,16} within projector augmented-wave (PAW) method,^{17,18} general gradient approximations (GGA)¹⁹ were used in the present calculations. The La($5s^25p^65d^16s^2$), Ni($3d^94s^1$), P($3s^23p^3$), O($2s^22p^4$) are treated as valence states. To ensure enough convergence, the energy cutoff was chosen to be 600 eV, and the Brillouin zone was sampled with a mesh of $16 \times 16 \times 8$ k points generated by the scheme of Monkhorst-Pack²⁰. A first order Methfessel-Paxton method with $\sigma = 0.2$ eV was used for relaxation. The crystal cell and internal parameters were optimized using the conjugate gradient method until the total forces on each ion less than 0.01 eV/Å. Then density of states (DOS) calculations were performed using the tetrahedron method with the Blöchl corrections²¹. The Fermi surfaces and 3D charge density iso-surfaces have been drawn by *Xcrysden*²².

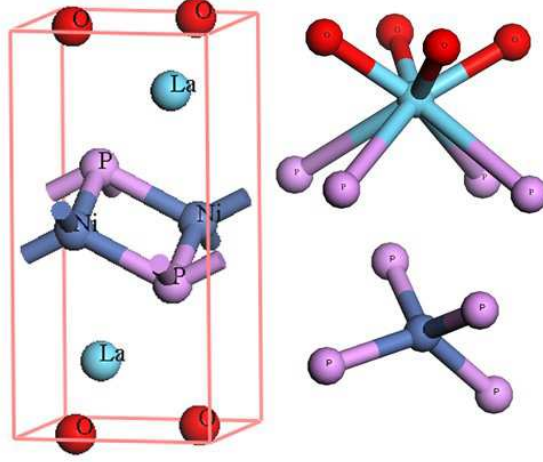


FIG. 1: Crystal structure of LaNiPO and near-neighbour coordinations of La and Ni atom. The element symbols have been labeled in the figure.

TABLE I: Comparison of experimental and calculated crystallographic Parameters of LaNiPO.

	a (Å)	c (Å)	z_1	z_2
Expt.1 ^a	4.0461	8.100	0.1531	0.626
Expt.2 ^b	4.0453	8.1054	0.1519	0.6257
Calculation	4.0353	8.2168	0.1513	0.6247

^aRef. 13.

^bRef. 14.

III. RESULTS AND DISCUSSION

A. Crystal Structure

LaNiPO crystallizes in the tetragonal ZrCuSiAs structure (space group $P4/nmm$) with the Ni atom at 2a (0.75, 0.25, 0), O at 2b (0.75, 0.25, 0.5), La at 2c (0.25, 0.25, z_1) and P at 2c(0.25, 0.25, z_2). It has a layered structure composed of an alternating stack of LaO and NiP block. The crystal structure is therefore rather simple with eight atoms (two formula units) in the unit cell as shown in Fig. 1. Lanthanum is eightfold coordinated by four oxygen and four phosphorus atoms. The nickel atoms are tetrahedrally coordinated by four phosphorus atoms, forming a distorted tetrahedra with two different P-Ni-P angles.^{13,14} And they also have four neighboring nickel atoms within the same layer.

Table I gives the optimal structural parameter of LaNiPO together with available experimental results. The experimental results are very consistent with each other. The present calculation is also in agreement with experiment, which indicates that the calculation is accurate. The slight difference between experiment and calculation may be induced by the fact that the LDA/GGA calculation cannot describe the electronic correlation between 3d electrons of Ni atom accurately. It seems that in order to give a more reasonable description, further calculation including the electronic correlation should be performed.

B. Density of States and Binding Properties

Fig. 2 shows the calculated total and partial DOS of LaNiPO. We can see the states below -13 eV is contributed by La and O atom. And the La-p and O-s shows strong hybridization with each other under the range -20 to -13 eV, indicating strong La-O bonding. The energy range from -12 to -10 eV is predominated by the P and Ni atoms with only a weak mixture of La atom. Whereas all atoms are contributing to the DOS at the energy range -6 to -3 eV. It should be noticed that from -2 to 2 eV, the 3d states of Ni atoms dominate the DOS, together with a slight contribution from P-3p states, while the La and O almost may be neglected. These results indicate that there are a significant overlap between the orbit in La-O and Ni-P and the bonding differs considerably from ionic ones.

As shown in above DOS analysis, we can find that the states of Ni and P atom predominate DOS near Fermi level, which

TABLE II: Electronic charges belonging to each atomic specie obtained by Bader analysis, compared with a purely ionic picture. The results of LaFePO taken from the Ref.²⁷ are included for comparison.

	La	M	P	O	LaO	MP
Bader(LaNiPO)	9.0902	9.9435	5.6841	7.2822	16.3724	15.6276
ionic picture(LaNiPO)	8(La ³⁺)	8(Ni ²⁺)	8(P ³⁻)	8(O ²⁻)	16(LaO ⁺)	16(NiP ⁻)
LaFePO ^a	9.05	7.59	6.05	7.31	16.36	13.64

^aRef. 27

suggests that the superconductivity origins from the contribution of the Ni 3d and P 3p as shown in Fig. 2(a). The layered copper-based superconductors have been extensively studied for several decades. In cuprate superconductors, Cu²⁺ occupies a planar 4-fold square site and the charge carriers at the Fermi level are driven by the $d_{x^2-y^2}$ orbit. While Ni²⁺ in LaNiPO occupies a tetrahedral site coordinated with four P³⁻ ions. Such a marked difference in the coordination structure between the LaNiPO and cuprate superconductor is expected to lead to the different mechanism of superconductivity. The Ni ion in LaNiPO is formally in a $3d^8$ configuration. In a tetrahedral crystal field, The Ni d bands will split into a lower lying e and an upper lying t_2 orbit. However, because of the distorted tetrahedral, as shown in Fig. 2(b) a clear separation in energy of the d orbit in a lower e ($3d_{z^2}$, $3d_{x^2-y^2}$) and higher t_2 ($3d_{xy}$, $3d_{yz}$, $3d_{xz}$) set is not seen in the present calculation. Whereas $3d_{xy}$ and $3d_{z^2}$ contributes more to DOS near the Fermi surface, which may play a more important role in superconductivity. In addition, from Fig. 2(b) and Fig. 2(c), all five 3d orbits of Ni atom and three p orbits of P atom has comparable contribution to DOS at the Fermi level.

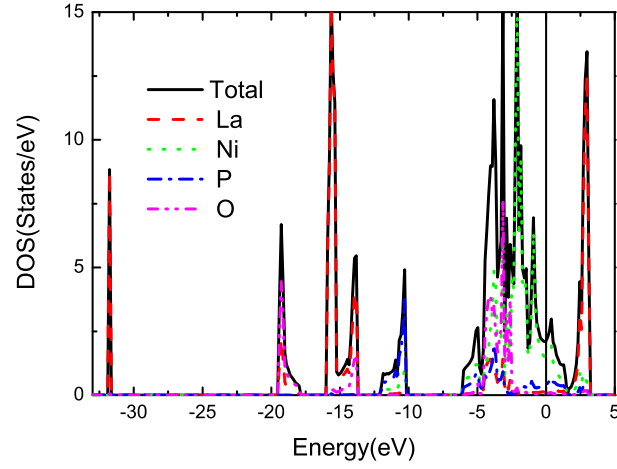
We also analysis the DOS using the concept of two-dimensional (2D) building blocks^{23,24,25,26}. It will be helpful to understand how charge transfer and hybridization effects will affect their electronic and binding properties when building the solid from these separated blocks. From the Fig. 3, we can see that the LaO states are pushed up in energy by approximately 2 eV, and becoming insulating in the solid but the isolated LaO layer is metallic, which indicate there are electron transfers from the LaO to NiP when building the solid. From the figure, we also conclude that the LaO-FeP interaction is strongly ionic character with weak hybridization under energy range of -5 and -2 eV.

As shown above, the qualitative electronic structure and binding properties is very similar to the results of LaFePO give in Ref. 27. In order to understand the binding properties more quantitatively, we also performed a Bader analysis^{28,29} of the charge density. The core charge missed in general pseudopotentials method has also been added to perform this analysis. Table II gives the charges of each atom specie using bader analysis together with the pure ionic picture. We can notice that the La-O and Ni-P bonds differ considerably from ionic character, whereas the bonding between the LaO and FeP blocks is mostly ionic. It is consistent with the previous DOS analysis. Compared with the result of LaFePO²⁷, we also find that the deviation of ionic character between Ni and P is larger than the case of LaFePO, which suggests the covalency between 3d metal and P atoms is stronger in LaNiPO.

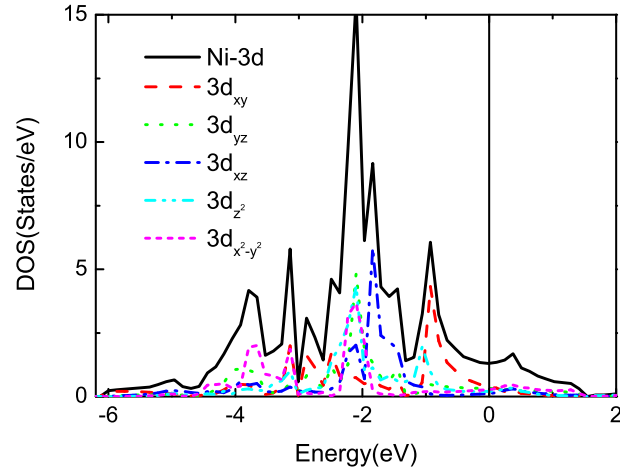
C. Band Structure and Fermi Surface

Now, Let's turn our attention to band structure. As shown in Fig. 4, the characteristic feature of band structures is the strongly pronounced two dimensionality along Γ -Z and A-M. We observe four bands across the Fermi energy, which have been indicated in the figure with different colors. The corresponding Fermi surface in the first Brillouin zone are displayed in Fig. 5. Due to the two-dimensional electronic structure, all Fermi surfaces are cylindrical-like sheets parallel to the k_z direction. The first sheet is centered along R-X whereas the other three are centered along the A-M high symmetry line. Such a series of Fermi surfaces are different from the results of LaFePO²⁷, where five bands across the Fermi level with four of them being cylindrical-like sheets (two along A-M and the other two along Γ -Z direction) and the other one being a distorted sphere along Γ -Z. The absence of distorted sphere Fermi surface sheet suggests the two dimensionality of band structure in LaNiPO is more pronounced than the case of LaFePO.

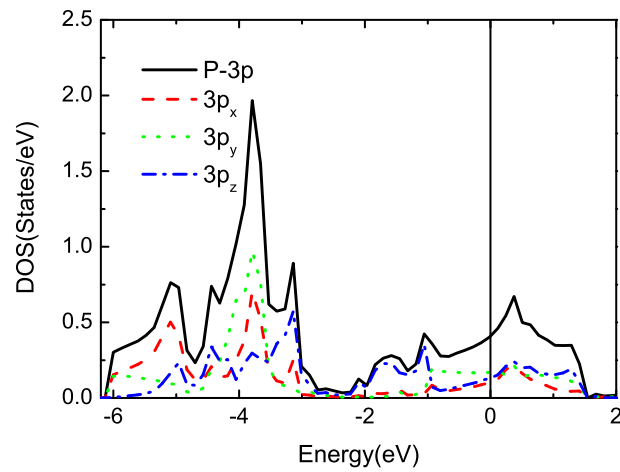
For further insight into the mechanism, we give the band decomposed charge density in Fig. 6. Although the Fermi surface of all bands have similar shape, the iso-surfaces of band decomposed charge density are different from each other as shown in Fig. 6 and Fig. 7, which also suggests that the orbital component is different. From the shape of iso-surface, we can speculate that the band *a* is made up of Ni- $3d_{xy}$ and weakly mixture with $p - \sigma$ orbit, which may be built with p_x and p_y . In case of the band *d*, the Ni orbit is mainly contributed by $3d_{x^2-y^2}$ and the states of P atom exhibit a p_z orbital character. It seems that the orbital component of band *b* and *c* is more complicated than *a* and *d*. Combined with different orbital picture, we can deduce the 3d orbital character of *c* is mostly contribute by $3d_{z^2}$ and maybe some component of $3d_{x^2-y^2}$. Whereas the band *b* may be mixed with $3d_{xz}$ and $3d_{yz}$, the states of P are similar to *a*, which may be composed of p_x and p_y . Our results shows that not only the $3d_{x^2-y^2}$ driving superconductor in layered copper-based oxides, but also all five 3d orbits are contribute to charge carriers at the Fermi level. So, it seems that the underlying mechanism is very complicated in ZrCuSiAs structured superconductor.



(a)



(b)



(c)

FIG. 2: Total density of states and Partial density of states for each atomic species(a) and the orbit resolved density of states for Ni 3d states(b) and P 3p states(c) of LaNiPO. The Fermi level is at zero energy.

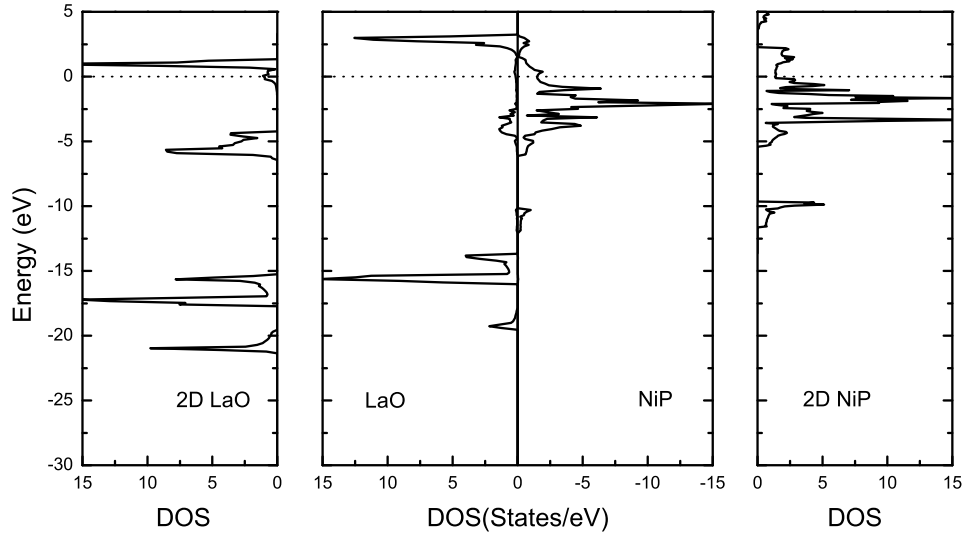


FIG. 3: Comparison of the DOS of the LaO(left) and NiP (right) blocks calculated as isolated entities with the PDOS for LaO (center left) and NiP (center right) in the LaNiPO solid.

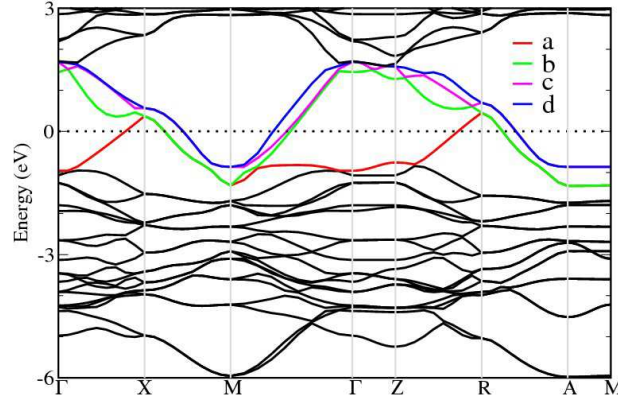


FIG. 4: The calculated band structure of LaNiPO. The Fermi level is at zero energy and marked by a horizontal dashed line. Four bands across the Fermi level are indicated in figure and marked with different colors.

IV. CONCLUSION

Based on First-principles calculation, we have investigated the electronic structure, binding properties and Fermi surface character of a new ZrCuSiAs structured superconductor LaNiPO. Our results indicate that the density of states and bonding properties are similar to the results of LaFePO. However, the Fermi surface character exhibits remarkable difference and two-dimensional character is more significant in case of LaNiPO. We also find that the orbital components of Fermi surfaces are very complicated, which suggests that the superconductivity mechanism is remarkably different from the well-known cuprate superconductors.

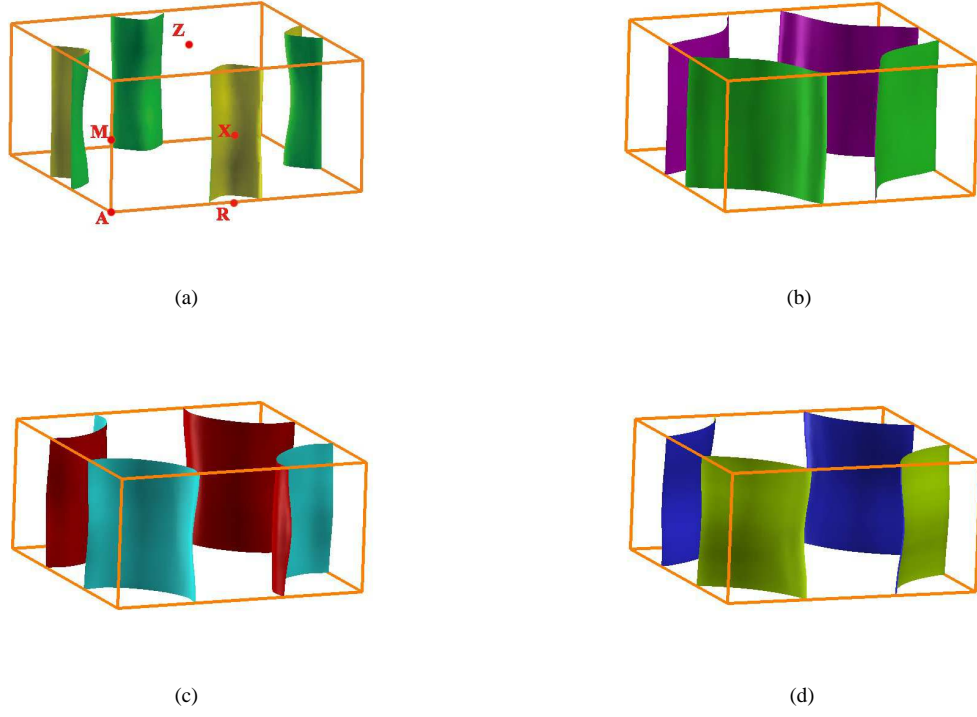


FIG. 5: The Fermi surface sheet of LaNiPO shown in the first Brillouin zone centered around the Γ point.

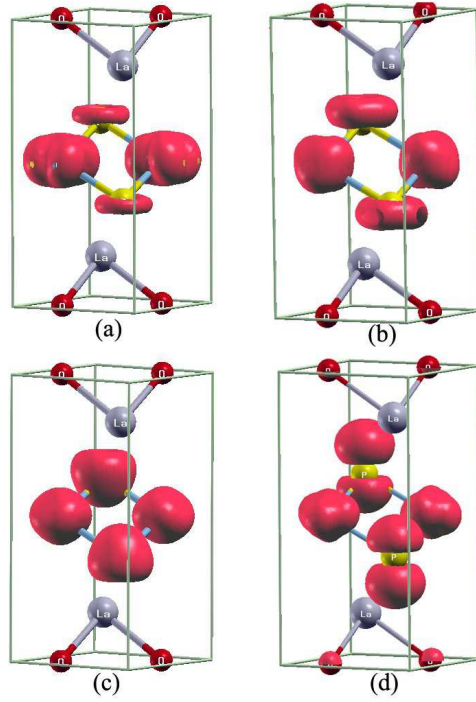


FIG. 6: The band decomposed charge density of four bands across the Fermi level. Iso surfaces correspond to $0.035 e/\text{\AA}^3$. In order to visualize the orbital character of P atoms, we choose $0.025 e/\text{\AA}^3$ for band *a*.

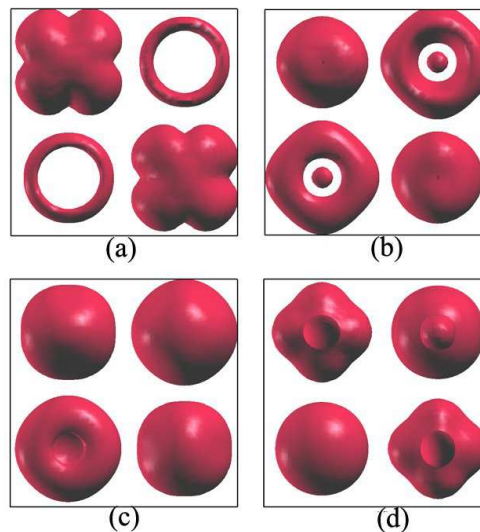


FIG. 7: Top view of the iso-surface of band decomposed charge density of four bands across the Fermi level. Iso surfaces correspond to $0.035 e/\text{\AA}^3$. In order to visualize the orbital character of P atoms, we choose $0.025 e/\text{\AA}^3$ for band *a*.

Acknowledgments

This work is supported in part by the Key Program of Educational Department (No: 07A070), Foundation of Natural Science, Hunan Province, China, and Scientific Research Foundation of Guangxi University (Grant No: X071117), China.

* Electronic address: tangbiyu@xtu.edu.cn

- ¹ V. Johnson and W. Jeitschko, J. Solid State Chem. **11**, 161 (1974).
- ² B. I. Zimmer, W. Jeitschko, J. H. Albering, R. Glaum, and M. Reehuis, J. Alloy. Compd. **229**, 238 (1995).
- ³ D. Kaczorowski, J. H. Albering, H. Noel, and W. Jeitschko, J. Alloy. Compd. **216**, 117 (1994).
- ⁴ J. H. Albering and W. Jeitschko, Z. Naturforsch., B: Chem. Sci. **51**, 257 (1996).
- ⁵ A. T. Nientiedt and W. Jeitschko, Inorg. Chem. **37**, 386 (1998).
- ⁶ Y. Takano, S. Komatsuzaki, H. Komasaki, T. Watanabe, Y. Takahashi, and K. Takase, J. Alloy. Compd. **451**, 467 (2008).
- ⁷ A. Nientiedt, W. Jeitschko, P. Pollmeier, and M. Brylak, Z. Nat.Forsch., B J. Chem. Sci. **52**, 560 (1997).
- ⁸ H. Kabbour, L. Cario, and F. Boucher, J. Mater. Chem **15**, 3525 (2005).
- ⁹ Y. Kamihara, H. Hiramatsu, M. Hirano, R. Kawamura, H. Yanagi, T. Kamiya, and H. Hosono, J. Am. Chem. Soc. **128**, 10012 (2006).
- ¹⁰ C. Y. Liang, R. C. Che, H. X. Yang, H. F. Tian, R. J. Xiao, J. B. Lu, R. Li, and J. Q. Li, Supercond. Sci. Tech. **20**, 687 (2007).
- ¹¹ C. Krellner, N. S. Kini, E. M. Bruning, K. Koch, H. Rosner, M. Nicklas, M. Baenitz, and C. Geibel, Phys. Rev. B **76**, 104418 (2007).
- ¹² C. Krellner and C. Geibel, eprint arXiv: 0709.4144 (2007).
- ¹³ T. Watanabe, H. Yanagi, T. Kamiya, Y. Kamihara, H. Hiramatsu, M. Hirano, and H. Hosono, Inorg. Chem. **46**, 7719 (2007).
- ¹⁴ M. Tegel, D. Bichler, and D. Johrendt, Solid State Sci. **10**, 193 (2008).
- ¹⁵ G. Kresse and J. Furthmüller, Comp. Mater. Sci. **6**, 15 (1996).
- ¹⁶ G. Kresse and J. Furthmüller, Phys. Rev. B **54**, 11169 (1996).
- ¹⁷ P. E. Blöchl, Phys. Rev. B **50**, 17953 (1994).
- ¹⁸ G. Kresse and D. Joubert, Phys. Rev. B **59**, 1758 (1999).
- ¹⁹ J. P. Perdew and Y. Wang, Phys. Rev. B **45**, 13244 (1992).
- ²⁰ H. J. Monkhorst and J. D. Pack, Phys. Rev. B **13**, 5188 (1976).
- ²¹ P. E. Blöchl, O. Jepsen, and O. K. Andersen, Phys. Rev. B **49**, 16223 (1994).
- ²² A. Kokalj, Comp. Mater. Sci. **28**, 155 (2003), code available from <http://www.xcrysden.org/>.
- ²³ O. M. Yaghi, M. O'Keeffe, N. W. Ockwig, H. K. Chae, M. Eddaoudi, and J. Kim, Nature **423**, 705 (2003).
- ²⁴ B. Chen, M. Eddaoudi, S. T. Hyde, M. O'Keeffe, and O. M. Yaghi, Science **291**, 1021 (2001).
- ²⁵ L. Cario, H. Kabbour, and A. Meerschaut, Chem. Mater. **17**, 234 (2005).
- ²⁶ H. Kabbour, L. Cario, M. Danot, and A. Meerschaut, Inorg. Chem. **45**, 917 (2006).
- ²⁷ S. Lebegue, Phys. Rev. B **75**, 035110 (2007).
- ²⁸ R. F. W. Bader, *Atoms in Molecules: A Quantum Theory* (Clarendon Press, 1990).
- ²⁹ G. Henkelman, A. Arnaldsson, and H. Jónsson, Comp. Mater. Sci. **36**, 354 (2006).